Int. J. Heat Mass Transfer. Vol. 28, No. 2, pp. 395–406, 1985
Printed in Great Britain

0017–9310/85 $3.00 + 0.00
Pergamon Press Ltd.

Temperature measurement and heat transfer in flowing polymer melts

J. VAN DAM and H. JANESCHITZ-KRIEGL*

Laboratory of Technology of Macromolecular Compounds, Delft University of Technology, Julianalaan 136, 2628 BL Delft, The Netherlands

(Dedicated to Prof. R. B. Bird, University of Wisconsin, on occasion of his 60th birthday)

(Received 15 *March* 1984)

Abstract—A theoretical description is given for the steady state heat transfer on a rod-like temperature probe inserted into a flowing polymer melt in an upstream direction. First the problem was solved numerically for a Newtonian and a power-law fluid. Local Nusselt numbers were obtained as functions of local Graetz numbers for a series of Péclet numbers. With the aid of the experience gathered, approximate analytical solutions were produced for low and high Graetz numbers, neatly matching in the intermediate range. The obtained simplified results enable a quick judgement of the usefulness of practical temperature measurements. A favourable comparison is made with Van Leeuwen's and own experimental results.

1. INTRODUCTION

IN POLYMER melt processing, measurement and control of temperatures are of great importance. In general, the temperature in the flowing polymer melt is different from that of the machine wall. This is mainly due to the very low heat conductivity of molten polymers. As a consequence, in many practical cases a local temperature measurement in the interior of the melt becomes desirable. This is carried out with a suitable temperature probe [1]. However, very often little space is left in the machine for the introduction of such a probe. The situation is complicated by the large mechanical forces exerted on the probe because of the high viscosity of the flowing melt. This means that one has to choose a rather short, thick probe, consisting of a metal tube (in general of stainless steel), in which one or more thermocouples are installed. The heat conduction through such a probe is relatively large compared with the heat conduction through the melt. As a consequence, a temperature will be measured which lies between the actual melt temperature and the temperature of the machine part in which the probe is mounted.

In this paper the development is given of a theory which enables the calculation of the actual melt temperature from the signal obtained on the temperature probe. The respective considerations are restricted to a cylindrical probe arranged in a direction parallel to the stream lines in the center of a duct. The tip of the probe is in an upstream direction, which means that the downstream end of the probe is considered to be mounted on a sturdy bridge or on the tip of a torpedo as used in extruders for pipe extrusion. For several reasons probes which are mounted in a direction perpendicular to the stream lines have not proven to be useful. First of all, they are exposed to strong bending forces [2]. Serious deformation and even fracture are the consequences. Secondly, there is a less clear situation as to the interpretation of the signal obtained, since in general the polymer melt temperature itself varies along such a probe. Thirdly, also the theoretical treatment is much more complicated.

The relation between the measured signal and the melt temperature is strongly dependent on the heat transfer between the streaming melt and the probe. For this reason a large part of this contribution is devoted to the description of this phenomenon. The results of the given theory are not only applicable to the problem of temperature measurement but have a more general significance in the field of heat transfer between a flowing polymer melt and a solid surface. On the other hand, a properly equipped temperature probe is particularly suitable for the determination of heat transfer coefficients [1, 2].

2. BASIC PRINCIPLE OF TEMPERATURE PROBE: HEAT BALANCE

In Fig. 1 a schematic drawing is given of the temperature probe in its upstream position. The probe which consists of a stainless steel tube of radius κR, wall thickness w and length L, is located along the centre line of a cylindrical tube of radius R. This tube represents the duct through which the polymer melt flows. In reality one has $\kappa \ll 1$. The tube is sealed in some way at its tip. There are two thermocouples in the interior of the probe, one in the tip ($z = 0$) measuring a temperature T_1, and another in the rear ($z = L$) giving a reference temperature T_2. This second thermocouple is not necessarily located at the junction where the probe is mounted on the mentioned bridge or torpedo.

* Present address: Johannes Kepler University Linz, A-4040 Linz, Austria.

NOMENCLATURE

a	thermal diffusivity [$m^2 s^{-1}$]
B	constant according to equation (20)
c	heat capacity [$J kg^{-1} K^{-1}$]
$f(\kappa)$	dimensionless shear rate at probe surface
F	ratio of dimensionless melt temperature and dimensionless probe temperature
$g(\kappa)$	dimensionless second derivative of flow profile at probe surface
G	reciprocal Graetz number
Gz	Graetz number
h	heat transfer coefficient [$J m^{-2} s^{-1} K^{-1}$]
$I_{-3/5}(x)$	Bessel function
k	thermal conductivity [$J m^{-1} s^{-1} K^{-1}$]
K	consistency index in power-law model [$N s^n m^{-2}$]
L	length of temperature probe (*viz.* distance between thermocouples) [m]
n	power-law index
Nu	Nusselt number
Pe	Péclet number
Pr	Prandtl number
r	radial coordinate [m]
R	radius of cylindrical duct [m]
Re	Reynolds number
T	temperature [K]
u	parameter in equations (30) and (32)
v_z	axial fluid velocity [$m s^{-1}$]
w	wall thickness of temperature probe [m]
x, y	auxiliary variables
z	axial coordinate [m].

Greek symbols

α, β	auxiliary variables (equation (24))
$\Gamma(a)$	complete gamma function
$\Gamma(a, x)$	incomplete gamma function
θ	dimensionless temperature
κ	ratio of the radii of probe and duct
ν	kinematic viscosity [$m^2 s^{-1}$]
ξ	dimensionless distance from the probe surface
ρ	density [$kg m^{-3}$]
τ_{rz}	shear stress [$N m^{-2}$]
ϕ	dimensionless fluid velocity
Φ	dependence of temperature difference over the probe length on the reference temperature.

Subscripts

0	values at small Graetz number
1	tip of probe
2	downstream reference thermocouple
c	probe
i	intersection
L	downstream distance of thermocouples
m	melt.

In that which follows it is assumed that the radius of the probe is so small compared with that of the cylindrical duct that the temperature of the latter duct (machine wall) is of no influence on the temperature of the probe. A more accurate formulation is that the penetration depth for the adjustment of the melt temperature to the duct wall temperature (Graetz number $\propto R^2$) is very much larger than the radius of the probe (Graetz number $\propto (\kappa R)^2$). This assumption is justified as in practice the ratio κ of the mentioned radii is almost always smaller than 0.15. This means that, in that which follows, the radius R of the duct is only used as an auxiliary parameter for the calculation of the velocity profiles.

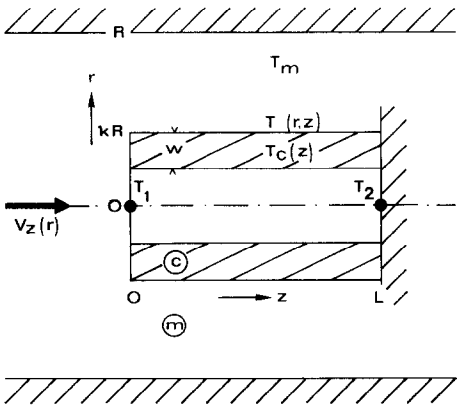

FIG. 1. Schematic drawing of the probe and its surroundings (not on scale).

In the steady state, when the temperature of the flowing melt does not vary with time, the energy balance for a longitudinal segment dz of the probe reads [1]:

$$k_c \frac{d^2 T_c}{dz^2} - \frac{2\kappa R}{w(2\kappa R - w)} h(T_c - T_m) = 0 \qquad (1)$$

where $T_c(z)$ is the temperature in the stainless steel tube of the probe, T_m is the undisturbed temperature of the flowing polymer melt (at a sufficient distance from the probe surface), k_c is the thermal conductivity of the stainless steel, and h is the heat transfer coefficient for transfer from the probe to the melt.

This heat balance consists of two terms. The first

term is the result of axial heat conduction within the wall of the stainless tube. The second term is the consequence of heat transfer from the probe to the melt (the denominator of the front factor actually belongs to the first term). In the derivation of equation (1) the following assumptions were made:

(a) The interior surface of the stainless steel tube is adiabatic (at $r = \kappa R - w$).
(b) The temperature T_c is homogeneous in the radial direction, i.e. over the thickness w of the tube wall. This assumption is certainly justified since $w \ll L$ and the thermal conductivity k_c of the metal is much larger than that of the polymer melt.

From the definition, the heat transfer coefficient h reads [3]:

$$h = -\frac{k_m}{T_c - T_m}\left(\frac{\partial T}{\partial r}\right)_{r=\kappa R} \tag{2}$$

where $T(r, z)$ is the temperature of the melt in the neighbourhood of the wall of the probe and k_m is the thermal conductivity of the melt.

For the calculation of the temperature distribution $T_c(z)$ in the probe or, in other words, for the solution of differential equation (1), the heat transfer coefficient h must be known as a function of z.

3. HEAT TRANSFER FROM FLOWING MELT TO PROBE SURFACE

According to equation (2) the temperature gradient in the melt obtained at the surface of the probe is required for the calculation of the heat transfer coefficient h. The temperature of the flowing melt results from a heat balance over the volume element $2\pi r\, dr\, dz$ [3]:

$$v_z \frac{\partial T}{\partial z} = \frac{a_m}{r}\frac{\partial}{\partial r}\left(r\frac{\partial T}{\partial r}\right) \tag{3}$$

where $a_m = k_m/\rho_m c_m$ is the thermal diffusivity of the melt, ρ_m is its density, c_m its heat capacity and v_z the local velocity of the melt (moving in the z-direction).

This equation holds under the following conditions:

(a) The flow is laminar since the Reynolds number $Re = 2\kappa R\langle v_z\rangle/\nu_m$ (with ν_m being the kinematic viscosity of the melt) is very small.
(b) The heat conduction in the z-direction is negligible compared with the heat convection in this direction. This is true only if the Péclet number $Pe = 2\kappa R\langle v_z\rangle/a_m$ is not too small, in other words, if the fluid velocity v_z is not too low. In Section 3.3 a more accurate treatment will be given for low Péclet numbers.
(c) The contribution of extra viscous heat (energy dissipation) generated in the polymer melt by the presence of the probe will be disregarded. In a recent paper Pittman and Mahmoudzadeh [4] present numerical calculations of the temperature distribution in an upstream probe and its surroundings, which indicate that the influence of viscous heating on tip temperature will seldom be significant in practice. However, along the side of the probe larger temperature rises can occur, at high flow rates; their effect on heat transfer needs further investigation.

With the aid of the dimensionless variables

$$\theta = (T - T_m)/(T_2 - T_m), \quad \theta_c = (T_c - T_m)/(T_2 - T_m)$$

Graetz number $Gz = (\kappa^2 R^2/a_m)(\langle v_z\rangle/z)$,

$$G = 1/Gz$$

Nusselt number $Nu = 2\kappa R h/k_m$

$$\xi = (r - \kappa R)/\kappa R \quad \text{and} \quad \phi = v_z/\langle v_z\rangle$$

one obtains instead of equations (3) and (2):

$$\phi\frac{\partial\theta}{\partial G} = \frac{1}{1+\xi}\frac{\partial}{\partial\xi}\left[(1+\xi)\frac{\partial\theta}{\partial\xi}\right] \tag{4}$$

$$Nu = -\frac{2}{\theta_c}\left(\frac{\partial\theta}{\partial\xi}\right)_{\xi=0}. \tag{5}$$

For solving the differential equation (3) one needs the velocity in the neighbourhood of the probe surface as a function of r and z. In the literature no data can be found on the hydrodynamic entrance region (developing flow profiles) into an annulus at low Reynolds numbers (creeping flow). In contrast, measurements and calculations are known for creeping flow into cylindrical tubes (see e.g. Atkinson *et al.* [5]). From these results we know that the hydrodynamic entrance length is of the order of the radius of the tube if this length is defined as the distance from the entrance where the fully developed velocity in the center of the tube is reached for 99%. In an annulus containing a very thin internal cylinder (when compared with the external cylinder) the hydrodynamic radius is not very much different from that of the external cylinder. For such an annulus one can expect that the hydrodynamic entrance length is also of the order of the radius R of the external cylinder (cylindrical duct).

However, for our purpose this value cannot be relevant. In the first instance, the claim of 99% is very stringent. In the second instance one has to realize that the above mentioned calculations of the entrance length are based on the assumption of a flat flow profile at the entrance, whereas in our case the flow profile in front of the tip of the probe exhibits a shape which is, for its greatest part, almost identical with the shape of the fully developed flow profile in the annulus. This is true because of the relatively small radius of the probe with respect to that of the cylindrical duct ($\kappa \simeq 0.1$). Finally, one notices that the fluid close to the probe surface reaches its final velocity much earlier (i.e. at a much shorter distance from the tip of the probe) than the fluid somewhere more in the middle of the stream. These considerations lead to the assumption that, for our purpose, the velocity distribution along the whole probe can be considered to be fully developed and thus independent of z, even at small values of this variable.

However, even if the velocity v_z is considered to be a pure function of r for all values of z, beginning at $z = 0$, equation (3) cannot be solved analytically. This holds even for the most simple, Newtonian fluid.

A good approximate solution can be obtained, however, with the aid of the concept of the thermal boundary layer. Whereas the hydrodynamic entrance length is extremely short, as we have just explained, the thermal entrance length is extremely long, at the same time. As a matter of fact, the latter length is proportional to the Péclet number $Pe = Re \cdot Pr$ where the Prandtl number $Pr = \nu_m/a_m$ is extremely large for polymer melts ($Pr \simeq 10^7$). As a consequence, the thickness of the thermal boundary layer remains very small over the modest length of the probe. In this boundary layer the temperature of the flowing melt changes from T_c at the probe surface to the undisturbed melt temperature T_m. In fact, boundary layer concepts are widely accepted.

3.1. *Heat transfer at probe surface of constant temperature (T_c = constant)*

The most restrictive approach to problems in convective heat transfer has been given by Lévêque [6]. This approximation is valid for the heat transfer to a metal wall of constant temperature. It is assumed that the boundary layer is so thin that the curvature of the probe surface can be disregarded. As a consequence, the use of cylindrical coordinates can be abandoned. Simple Cartesian coordinates are serving the purpose. At the same time it is assumed that, within the thermal boundary layer, the velocity profile can be approximated by a straight line starting with zero at the probe surface. With these simplifications equation (4) becomes:

$$2f(\kappa)\xi \frac{\partial\theta}{\partial G} = \frac{\partial^2\theta}{\partial\xi^2} \tag{6}$$

where $f(\kappa)$ is the (dimensionless) velocity gradient at the probe surface:

$$f(\kappa) = \frac{\kappa R}{2\langle v_z\rangle}\left(\frac{dv_z}{dr}\right)_{r=\kappa R} = \frac{1}{2}\left(\frac{d\phi}{d\xi}\right)_{\xi=0}.$$

The variable $f(\kappa)$ is, apart from being a function of κ, also dependent on the rheological constitutive equation of the melt. Polymer melts can be described for many practical purposes by the Ostwald–de Waele or power-law model. For cylindrical flow symmetry this model reads:

$$\tau_{rz} = -K(dv_z/dr)^n \tag{7}$$

where τ_{rz} is the shear stress, K the consistency index and n the power-law index. For our purpose K and n are considered to be independent of the temperature.

It appears that $f(\kappa)$ is independent of K. It depends only on κ and the power-law index n. For a Newtonian fluid ($n = 1$) one has for developed flow in an annulus [3]:

$$f(\kappa) = \frac{1-\kappa^2-2\kappa^2\ln(1/\kappa)}{(1+\kappa^2)\ln(1/\kappa)-(1-\kappa^2)}.$$

A method for the calculation of $f(\kappa)$ for other values of n has been given by Fredrickson and Bird [7]. In Fig. 2 curves of $f(\kappa)$ are given for $n = 1$ and $n = 0.5$.

With the boundary conditions $\theta = 0$ at $G = 0, \theta = \theta_c$ at $\xi = 0$ and $\theta = 0$ at $\xi = \infty$, *viz.* at a sufficient distance from the probe surface, the solution of equation (6) reads:

$$\theta = \theta_c \frac{\Gamma(\frac{1}{3}, \frac{2}{9}f(\kappa)\xi^3/G)}{\Gamma(\frac{1}{3})} \tag{8}$$

where $\Gamma(a,x)$ is the incomplete gamma function $\int_x^\infty e^{-t}t^{a-1}\,dt$ and $\Gamma(a)$ is the complete gamma function $\int_0^\infty e^{-t}t^{a-1}\,dt$.

With the aid of equation (5) one obtains with this solution an expression for the dimensionless heat transfer coefficient (Nusselt number):

$$Nu = \frac{1}{\Gamma(\frac{4}{3})}\left[\frac{16}{9}f(\kappa)\right]^{1/3} Gz^{1/3}. \tag{9}$$

For temperature measurements in plastics processing this approximation appears to be not good enough, however. In extrusion practice Graetz numbers for typical probes are of the order of 0.5 to 100. In the boundary layer concept the ratio between thermal boundary layer thickness and probe diameter is given by $Gz^{-1/3}$. This means that the boundary layer thickness is of the order of magnitude of the diameter of the probe and that the curvature of the probe surface may not be disregarded.

A higher and better approximation can be obtained

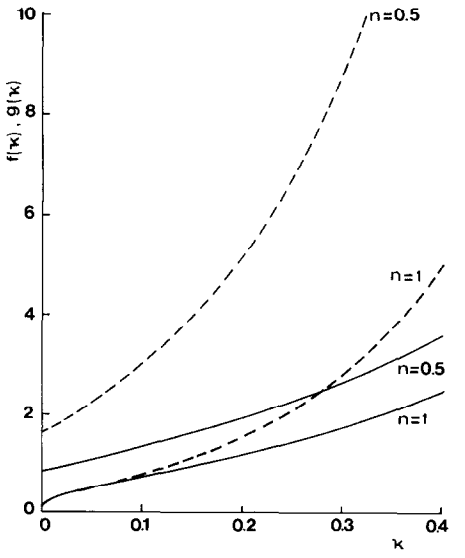

FIG. 2. Dependences of functions $f(\kappa)$ (———) and $g(\kappa)$ (– – –) on ratio κ for power-law index $n = 1$ (Newtonian fluid) and $n = 0.5$.

with the aid of a method, as developed by Richardson [8] for the flow of power-law fluids through cylindrical tubes. With this method cylindrical coordinates are used instead of Cartesian coordinates, as applied in the case of Lévêque's approach. In addition, not only the linear term of the velocity profile but also a quadratic term is taken into account for the calculation:

$$\phi(\xi) = 2f(\kappa)\xi - g(\kappa)\xi^2. \tag{10}$$

As the function $f(\kappa)$, also the new function $g(\kappa)$ does not depend on the consistency index K of the power-law fluid. For a Newtonian fluid ($n = 1$) one has as an example:

$$g(\kappa) = \frac{1-\kappa^2+2\kappa^2\ln(1/\kappa)}{(1+\kappa^2)\ln(1/\kappa)-(1-\kappa^2)}.$$

Also $g(\kappa)$ is shown in Fig. 2 as a function of κ for two power-law indices, $n = 1$ and $n = 0.5$.

Equation (4) becomes in this approximation:

$$[2f(\kappa)\xi - g(\kappa)\xi^2]\frac{\partial\theta}{\partial G} = \frac{1}{1+\xi}\frac{\partial}{\partial\xi}\left[(1+\xi)\frac{\partial\theta}{\partial\xi}\right]. \tag{11}$$

In order to simplify the solution of this equation the new dimensionless variables $y = \xi/G^{1/3}$ and $x = G^{1/3}$ are introduced. With these variables equation (11) reads:

$$\tfrac{1}{3}y(1+xy)[2f(\kappa)-g(\kappa)xy]\left(x\frac{\partial\theta}{\partial x} - y\frac{\partial\theta}{\partial y}\right) = x\frac{\partial\theta}{\partial y} + (1+xy)\frac{\partial^2\theta}{\partial y^2} \tag{12}$$

subject to the following boundary conditions: $\theta = 0$ at $x = 0$, $\theta = \theta_c$ at $y = 0$ and $\theta = 0$ at $y = \infty$.

It is now assumed that $\theta(x, y)$ can be written as:

$$\theta(x, y) = \theta_0(y) + \theta_1(y)x + \cdots. \tag{13}$$

In fact, a small value of x holds if the average speed of the fluid $\langle v_z\rangle$ is rather large, which means that the deviation from Lévêque's solution will be rather small. If the expression for θ, as given by equation (13), is introduced into equation (12), and if the terms of equal power of x are equated, one obtains:

$$\theta_0'' + \tfrac{2}{3}f(\kappa)y^2\theta_0' = 0 \tag{14}$$

and

$$\begin{aligned}\theta_1'' + \tfrac{2}{3}f(\kappa)y^2\theta_1' - \tfrac{2}{3}f(\kappa)y\theta_1 &= -y\theta_0'' - [1+\tfrac{1}{3}\{2f(\kappa)-g(\kappa)\}y^3]\theta_0' \\ &= -\{1-\tfrac{1}{3}g(\kappa)y^3\}\theta_0'\end{aligned} \tag{15}$$

where primes denote differentiation with respect to y.

Equation (14) furnishes the zeroth order approximation, *viz.* the Lévêque solution:

$$\theta_0 = \theta_c\frac{\Gamma(\frac{1}{3}, \frac{2}{9}f(\kappa)y^3)}{\Gamma(\frac{1}{3})}. \tag{16}$$

After introducing this zeroth order approximation θ_0 into equation (15) one obtains as a solution of this latter equation:

$$\begin{aligned}\theta_1 &= \theta_c\frac{g(\kappa)}{5\Gamma(\frac{4}{3})[6f(\kappa)]^{2/3}}y^2\,e^{-2f(\kappa)y^3/9} - \frac{1}{2}\left[1-\frac{1}{5}\frac{g(\kappa)}{f(\kappa)}\right]y\theta_0 \\ &= -\frac{1}{10}\frac{g(\kappa)}{f(\kappa)}y^2\theta_0' - \frac{1}{2}\left[1-\frac{1}{5}\frac{g(\kappa)}{f(\kappa)}\right]y\theta_0.\end{aligned} \tag{17}$$

This solution furnishes together with equation (5) the Nusselt number:

$$\begin{aligned}Nu &= -\frac{2}{\theta_c}\left[\left(\frac{\partial\theta_0}{\partial\xi}\right)_{\xi=0} + \left(\frac{\partial\theta_1}{\partial\xi}\right)_{\xi=0}G^{1/3}\right] \\ &= -\frac{2}{\theta_c}[(\theta_0')_{y=0}G^{-1/3} + (\theta_1')_{y=0}] \\ &= \frac{1}{\Gamma(\frac{4}{3})}\left[\frac{16}{9}f(\kappa)\right]^{1/3}Gz^{1/3} + \left[1-\frac{1}{5}\frac{g(\kappa)}{f(\kappa)}\right].\end{aligned} \tag{18}$$

3.2. *Heat transfer at probe surface of adapted temperature* ($T_c = T_c(z)$)

The theory described in Section 3.1 gives the heat transfer from the flowing melt to a cylindrical wall of constant temperature. However, if the temperature of the flowing melt is measured with a probe of not too great a length, the temperature T_c varies with the distance z from the tip. This dependence is determined by equation (1), which reads after the introduction of dimensionless variables:

$$\frac{d^2\theta_c}{dG^2} - B\,Pe^2\,Nu\,\theta_c = 0 \tag{19}$$

where

$$B = \frac{(\kappa R)^2}{4w(2\kappa R - w)}\frac{k_m}{k_c}. \tag{20}$$

The boundary conditions are: $d\theta_c/dG = 0$ at $G = 0$ ($z = 0$) and $\theta_c = 1$ at $G = G_L$ ($z = L$).

For an exact calculation of temperature profiles and heat transfer coefficients the set of equations (19), (4) and (5) must be solved simultaneously. This can be carried out only numerically. Some results of such a calculation, using an iterating finite difference method, are reproduced in Fig. 3 where the local Nusselt number is plotted against the local Graetz number (reciprocal dimensionless distance from the tip of the probe) for some values of the power-law index and the Péclet number.

In Fig. 4 the average Nusselt number $\langle Nu\rangle$, as obtained by averaging over the length of the probe, is plotted as a function of the Graetz number Gz_L as related to the total probe length L. One has:

$$\langle Nu\rangle = \frac{1}{L}\int_0^L Nu(z)\,dz = \frac{1}{G_L}\int_0^{G_L} Nu(G)\,dG$$

and

$$Gz_L = \frac{1}{G_L} = \frac{(\kappa R)^2}{a_m}\frac{\langle v_z\rangle}{L}.$$

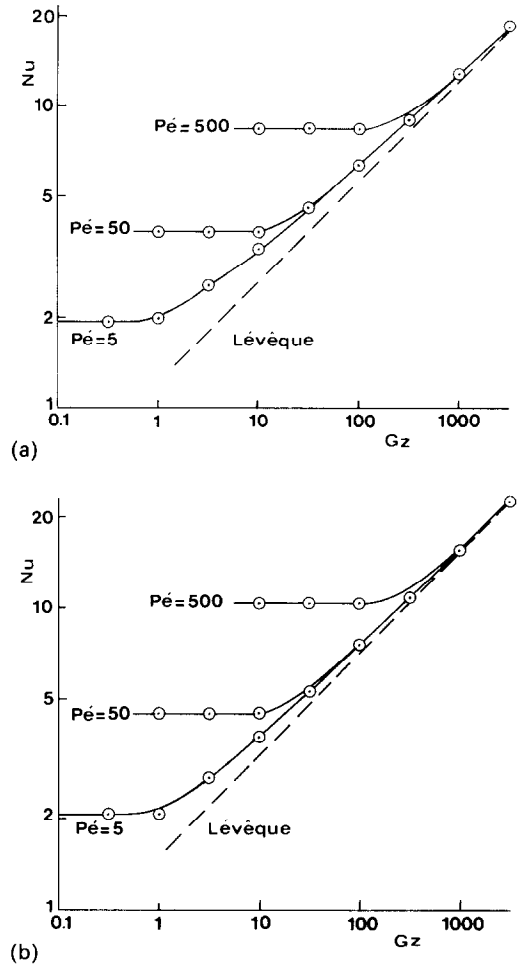

FIG. 3(a). Local Nusselt number Nu as a function of local Graetz number Gz for various Péclet numbers Pe as parameters, as obtained for $\kappa = 0.1$, $B = 5 \cdot 10^{-3}$ and $n = 1$ (Newtonian fluid); ⊙...approximation according to equations (25). (b) Local Nusselt number Nu as a function of local Graetz number Gz for various Péclet numbers Pe as parameters, as obtained for $\kappa = 0.1$, $B = 5 \cdot 10^{-3}$ and power-law index $n = 0.5$; ⊙...approximation according to equations (25).

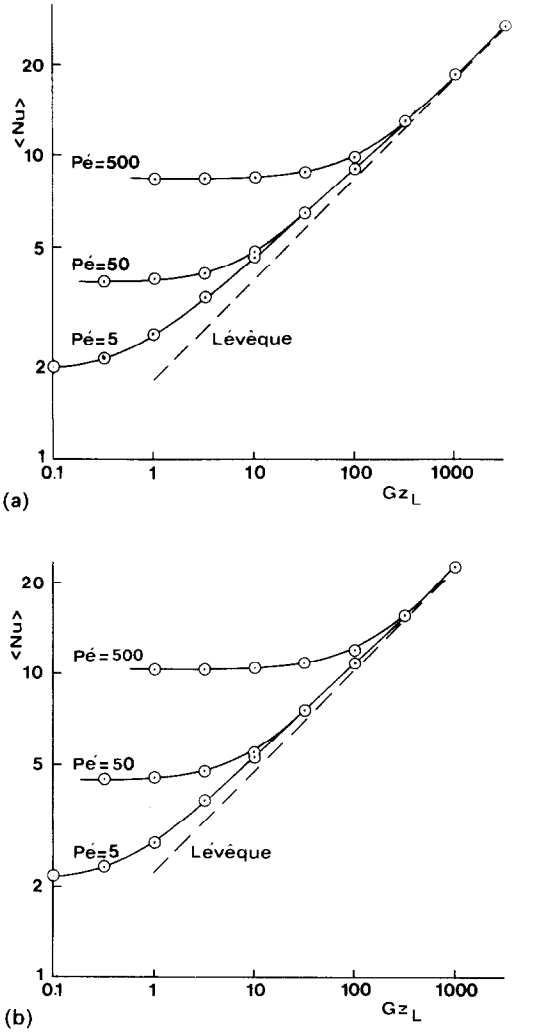

FIG. 4(a). Average Nusselt number $\langle Nu \rangle$ as a function of the Graetz number Gz_L related to the total length of the probe for various Péclet numbers as parameters, as obtained for $\kappa = 0.1$, $B = 5 \cdot 10^{-3}$ and $n = 1$ (Newtonian fluid); ⊙...approximation according to equations (27). (b) Average Nusselt number $\langle Nu \rangle$ as a function of the Graetz number Gz_L related to the total length of the probe for various Péclet numbers as parameters, as obtained for $\kappa = 0.1$, $B = 5 \cdot 10^{-3}$ and power-law index $n = 0.5$; ⊙...approximation according to equations (27).

This average Nusselt number is the quantity which is measured in practice, if a temperature probe with two thermocouples is used [1, 2].

By taking into account the dependence of T_c on z one obtains curves which level off at constant Nusselt numbers Nu_0 at small values of Gz and Gz_L. It is possible to give an analytical calculation of these 'developed' Nu_0 values.

Before doing so we notice that the local Nusselt numbers, as calculated in Section 3.1 for constant probe temperature (see equation (18)), are in surprising agreement with those calculated numerically, by solving equations (19), (4) and (5) simultaneously, as far as the non-horizontal parts of the full lines (at sufficiently large Graetz numbers) are concerned (see the inserted open circles). A discussion of this apparent usefuless of the 'constant probe temperature approximation' will be given in Section 4. For the moment, another approximation, *viz.* the 'constant Nusselt number approximation' will be given. This approximation appears to be useful for the horizontal parts of the curves of Fig. 3.

For $G \to \infty$ (large z, small Gz) and constant Nu ($= Nu_0$) equation (19) has the simple solution:

$$\theta_c = c_1 e^{(BPe^2 Nu_0)^{1/2} G} + c_2 e^{-(BPe^2 Nu_0)^{1/2} G} \simeq c_1 e^{(BPe^2 Nu_0)^{1/2} G}.$$

If the boundary condition $\theta_c = 1$ is inserted for $G = G_L$, one obtains:

$$\theta_c = e^{-(BPe^2 Nu_0)^{1/2} (G_L - G)}. \quad (21)$$

The following factorization is now tried:

$$\theta(\xi, G) = \theta_c(G) \cdot F(\xi, G).$$

If this is inserted into equation (4) one obtains:

$$\phi F \frac{d\theta_c}{dG} + \phi\theta_c \frac{\partial F}{\partial G} = \frac{\theta_c}{1+\xi} \frac{\partial}{\partial \xi}\left[(1+\xi)\frac{\partial F}{\partial \xi}\right].$$

From equation (21) one obtains $d\theta_c/dG = (BPe^2Nu_0)^{1/2}\theta_c$. If this is inserted into the last equation, θ_c can be eliminated as a common factor of all terms. In this way one retains:

$$\frac{1}{1+\xi}\frac{\partial}{\partial \xi}\left[(1+\xi)\frac{\partial F}{\partial \xi}\right] - (BPe^2Nu_0)^{1/2}\phi F - \phi\frac{\partial F}{\partial G} = 0,$$

or, after substituting G by $1/Gz$:

$$\frac{1}{1+\xi}\frac{\partial}{\partial \xi}\left[(1+\xi)\frac{\partial F}{\partial \xi}\right] - (BPe^2Nu_0)^{1/2}\phi F - \phi Gz^2\frac{\partial F}{\partial Gz} = 0.$$

For $Gz \to 0$ the last term is negligible. As a result for small values of Gz the function F appears to depend on ξ only:

$$\frac{1}{1+\xi}\frac{d}{d\xi}\left[(1+\xi)\frac{dF}{d\xi}\right] - (BPe^2Nu_0)^{1/2}\phi F = 0. \quad (22)$$

Because of the boundary condition $\theta = \theta_c$ for $\xi = 0$ one has $F(0) = 1$.

For a sufficiently large value of ξ one has $\theta = 0$, which means that $F(\infty) = 0$. Using these boundary conditions one can easily solve equation (22) by means of an expansion into a series or, faster, by a numerical technique. The Nusselt number Nu_0 follows finally from:

$$Nu_0 = -2\left(\frac{dF}{d\xi}\right)_{\xi=0}.$$

In the range of higher Péclet numbers an asymptotic solution of equation (22) may facilitate the calculation of Nu_0. This asymptotic solution, which can be derived using the method of Olver [9], leads to the following expression for Nu_0:

$$Nu_0 = [\Gamma(\tfrac{2}{3})\alpha B^{1/6}]^{6/5} Pe^{2/5} + \tfrac{6}{5}\beta \quad (23)$$

where α and β are constants, which also appear in equation (18):

$$\alpha = \frac{1}{\Gamma(\frac{4}{3})}\left[\frac{16}{9}f(\kappa)\right]^{1/3} \quad \text{and} \quad \beta = 1 - \frac{1}{5}\frac{g(\kappa)}{f(\kappa)}. \quad (24)$$

For $Pe = 1000$ the accuracy of the asymptotic approximation is of the order of 0.2%, for $Pe = 100$ about 1% and for $Pe = 10$ about 5%. In practice Pe values smaller than 10 are seldom encountered.

In Fig. 5 a graphical representation is given of Nu_0 as a function of the Péclet number for a Newtonian fluid and for a power-law fluid with power-law index 0.5. The higher the axial convection (the higher Pe), the larger is the constant Nusselt number Nu_0 which governs the heat transfer at a large distance from the tip of the probe (large as compared with the probe diameter).

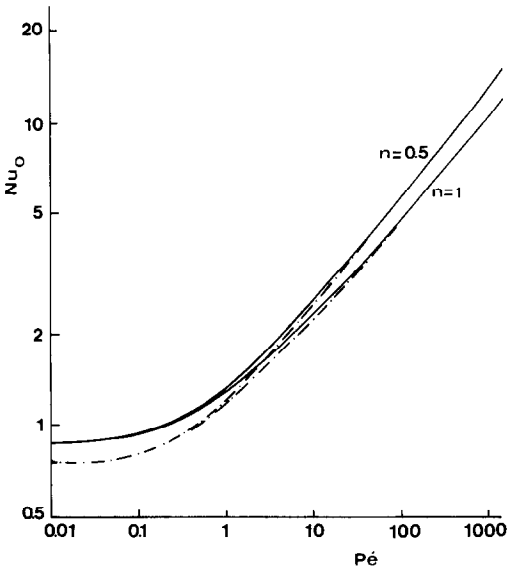

FIG. 5. Developed Nusselt number Nu_0 as a function of Péclet number Pe for a Newtonian fluid ($n = 1$) and for a power-law fluid with $n = 0.5$. ——— without correction for axial conduction in the melt; —·—·— axial heat conduction in the melt incorporated in the calculations. Plot constructed for $\kappa = 0.1$ and $B = 5 \cdot 10^{-3}$.

In Fig. 5 the Nusselt number Nu_0 is also drawn for the cases where the axial heat conduction is taken into account in addition to the axial heat convection. The corresponding functions are indicated by dashed lines (in equations (3) and (4) this conduction is disregarded). One notices that for accurate measurements this correction becomes of importance for $Pe < 10$ (see next section).

We now have two approximations for the local Nusselt number as a function of the local Graetz number, which read:

$$\left.\begin{aligned} Nu &= \alpha Gz^{1/3} + \beta \quad \text{for} \quad Gz \geqslant Gz_i \\ Nu &= Nu_0 \quad\quad\quad\;\; \text{for} \quad Gz \leqslant Gz_i \end{aligned}\right\} \quad (25)$$

where α and β are defined in equations (24). These approximations give a description which is sufficiently accurate for practical purposes.

The value of Gz_i is given by the Graetz number at the intersection of these two approximations:

$$Gz_i = \left(\frac{Nu_0 - \beta}{\alpha}\right)^3. \quad (26)$$

In Fig. 3 a number of points (open circles) is introduced. These points are calculated according to the indicated concept of approximation. For the curves of $\langle Nu \rangle$ vs Gz_L this approximate description offers an even better agreement with the exact results, because of the integration. The dependence of $\langle Nu \rangle$ on Gz_L can be derived from the relation between Nu and Gz in the

following way:

$Gz_L \geqslant Gz_i$ (or $G_L \leqslant G_i$):

$$\langle Nu\rangle = \frac{1}{G_L}\int_0^{G_L}(\alpha G^{-1/3}+\beta)\,dG = \tfrac{3}{2}\alpha G_L^{-1/3}+\beta$$

$$= \tfrac{3}{2}\alpha G z_L^{1/3}+\beta, \qquad (27a)$$

$Gz_L \leqslant Gz_i$ (or $G_L \geqslant G_i$)

$$\langle Nu\rangle = \frac{1}{G_L}\left[\int_0^{G_i}(\alpha G^{-1/3}+\beta)\,dG+\int_{G_i}^{G_L} Nu_0\,dG\right]$$

$$= \frac{G_i}{G_L}(\tfrac{3}{2}\alpha G_i^{-1/3}+\beta)+\frac{G_L-G_i}{G_L}Nu_0$$

$$= Nu_0+\frac{\alpha^3}{2(Nu_0-\beta)^2}Gz_L. \qquad (27b)$$

Also in the graphs showing $\langle Nu\rangle$ vs Gz_L (Fig. 4) the points, as calculated according to the indicated way of approximation, are inserted as open circles. The agreement with the numerically calculated full lines can be considered as very good.

3.3. *Influence of axial heat conduction*

In the calculations carried out so far the contribution of axial heat conduction has not been taken into account. The influence of this conduction, in relation to the axial convection, is expressed by the Péclet number. If this number is small, the axial conduction cannot be disregarded. The following relation holds between the Graetz number and the Péclet number:

$$Gz = \frac{\kappa R}{2z}Pe.$$

A small Graetz number Gz (characteristic for the horizontal asymptote of the Nu–Gz relation), however, does not automatically mean a small Péclet number Pe. In fact, a small Gz is also obtained if z is large compared with κR (as is the case with a relatively long probe). The best manner for estimating the influence of axial conduction is given by a direct calculation of the Péclet number according to $Pe = 2\kappa R\langle v_z\rangle/a_m$. In practice reasonable values for the variables of the Péclet number are: $\kappa R = 10^{-3}$ m, $a_m = 10^{-7}$ m^2 s^{-1}. This means that even for average fluid velocities between $0.5\cdot 10^{-3}$ and $1.0\cdot 10^{-3}$ ms^{-1} the Péclet number is still considerably larger than one. In other words, axial heat conduction becomes of importance only if the flow almost stops. Even in this case the contribution of axial conduction must be observed only for the horizontal, asymptotic part of the Nu–Gz relation at small values of Gz.

In the heat balance, as given by equation (3), an extra term $a_m\partial^2 T/\partial z^2$ must be added on the right side to account for the contribution of the axial conduction. The dimensionless equation (4) then becomes:

$$\phi\frac{\partial\theta}{\partial G} = \frac{1}{1+\xi}\frac{\partial}{\partial\xi}\left[(1+\xi)\frac{\partial\theta}{\partial\xi}\right]+\frac{4}{Pe^2}\frac{\partial^2\theta}{\partial G^2}. \qquad (28)$$

A consideration for small values of Gz, analogous to that applied on equation (4) of Section 3.2, yields instead of equation (22):

$$\frac{1}{1+\xi}\frac{d}{d\xi}\left[(1+\xi)\frac{dF}{d\xi}\right]$$

$$-(BPe^2Nu_0)^{1/2}\phi F+4BNu_0F = 0. \qquad (29)$$

As equation (22) also this equation can easily be solved by the application of a series expansion or numerically. As a consequence of the contribution of axial conduction the Nu_0 values shift to somewhat lower values. As becomes obvious from Fig. 5, the influence of this conduction becomes noticeable at Péclet numbers smaller than 10. A critical value of Pe of the order of one is reasonable in view of the restricted accuracy of most practical measurements, however.

4. TEMPERATURE IN THE PROBE

If the relation between the local Nusselt and Graetz numbers (or between h and z) is known (or assumed), the corresponding temperature distribution along the probe follows with the aid of equation (1) or its dimensionless form (19) from the imposed boundary conditions at $z = 0$ and $z = L$. If, in particular, equations (19), (4) and (5) are solved simultaneously by a numerical technique, the obtained solution obviously contains θ_c as a function of G.

For that which follows the results of our two limiting cases, of the 'constant Nusselt number approach' and of the 'constant probe temperature approach', are of particular interest. Whereas the postulate of the first approach is of a nature included in the consideration of the first paragraph of this Section (i.e. the Nusselt number is *assumed* for the whole length of the probe), this is not the case with the postulate of the second approach. The pertinent Nusselt number dependence *follows* from this postulate. Moreover, if the temperature of the probe is assumed to be constant, one cannot easily derive a temperature profile for the probe. For this reason, the original postulate of the second approach is replaced by the postulate that the approximate result for Nu, as presented in its most simple form by Lévêque's law (i.e. $Nu \propto Gz^{1/3}$ or $h \propto z^{-1/3}$), takes over the leading role: it is *assumed* to hold for the whole probe length. At the same time, naturally, the condition of constant temperature along the whole probe must be released. In the range of variables where Lévêque's law holds well, it turns out that the greatest part of the probe is actually at a constant temperature. Only in the vicinity of the place where the probe is mounted to a machine part, bridge, etc., one must allow for noticeable temperature gradients.

Since the constant Nusselt number assumption and Lévêque's law, or more accurately its improved version as given by equation (18), appear to form useful approximations in the low and high Graetz number range, respectively, it clearly makes sense to ask for the temperatures in the probe which are the consequences of these approximations.

The temperatures in the probe are represented by the tip temperature T_1 and the temperature T_2 at a distance L downstream from the tip, while

$$\Phi = -\frac{d(T_1 - T_2)}{dT_2}$$

is a measure for the dependence of T_1 on (adjustable) T_2. With the assumption of constant Nusselt number one finds [1]:

$$\Phi = 1 - \frac{1}{\cosh u} \tag{30}$$

where the function u is defined as:

$$u = (BPe^2\langle Nu\rangle)^{1/2}/Gz_L = (B\langle Nu\rangle)^{1/2}\frac{2L}{\kappa R}. \tag{31}$$

If $Nu \propto Gz^{1/3}$ is assumed, one finds:

$$\Phi = 1 - \frac{1}{(\frac{6}{25})^{3/10}\Gamma(\frac{2}{5})u^{3/5}I_{-3/5}(\frac{2\sqrt{6}}{5}u)} \tag{32}$$

where $I_{-3/5}(x)$ is the modified Bessel function of the second kind of order 3/5.

The dependences of Φ on u for the two limiting cases are depicted in Fig. 6.

The full line between the two limiting curves is the result of a number of complete numerical calculations, for which the average value of Φ is plotted against u. These complete calculations were carried out for various values of the power-law index n, the ratio κ, the quantities B and Pe. It turns out to be impossible to fit the individual Φ-values to a master curve. But on the scale of Fig. 6 the individual curves of Φ vs u are so close together that they cannot be discerned. This also shows that $\Phi(u)$ is very insensitive for details in the assumptions.

As a conclusion the following may be stated: the original method [1] by which the average Nusselt number $\langle Nu\rangle$ on the probe is obtained with the aid of equation (30) from proper measurement of T_1 and T_2 is substantiated by the present calculations. One of the present authors [1] has proposed this method about twenty years ago and stimulated Van Leeuwen [2] to carry out his extremely successful measurements which are well known and will be rediscussed in the next Section.

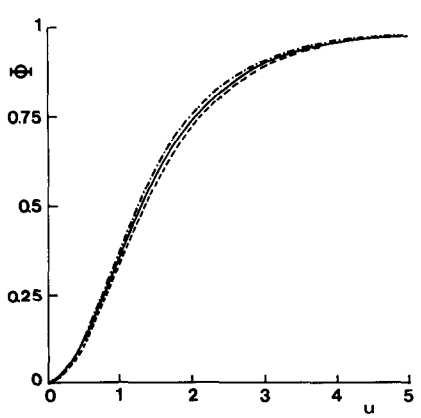

FIG. 6. Dimensionless temperature difference Φ as a function of variable u; ——— Nu constant over the whole length of probe; —·—·— Nu proportional to $Gz^{1/3}$ over the whole length of probe; ——— correct relation between Nu and Gz.

5. COMPARISON WITH EXPERIMENTAL DATA

The usefulness of the presented theory can be checked on the basis of dimensionless heat transfer coefficients $\langle Nu\rangle$ as determined experimentally with the aid of a compensation probe as described by Janeschitz-Kriegl *et al.* [1]. In such a probe reference temperature T_2 can be varied by a local (electric) heating of (air) cooling installed in the interior of the probe near thermocouple no. 2. In this way one obtains $T_1 - T_2$ as a function of T_2 in a given flow situation. This relation appears to be represented by a nice straight line in all practical situations investigated. This means that the slope of this line, *viz.* $\Phi = -d(T_1 - T_2)/dT_2$, can always be determined accurately. With the aid of Fig. 6 the corresponding value of u is easily obtained. The values of u are most accurate if Φ is of the order of one-half [1]. If this is not the case, a probe of adapted dimensions must be used. If Gz_L, Pe and B (from equation (20)) are known, $\langle Nu\rangle$ can be calculated with the aid of equation (31).

A unique series of measurements of $\langle Nu\rangle$ has been published by Van Leeuwen [2]. For a low density polyethylene in a temperature range between 160°C and 200°C this author has published values for $\langle Nu\rangle$ as determined for a great variety of flow conditions and appropriately dimensioned temperature probes. The B-values varied from $1.5 \cdot 10^{-3}$ to $7.5 \cdot 10^{-3}$, the Pe-numbers between 2 and 1000, and the Gz_L-numbers between 0.1 and 80.

As a consequence of the great variety of B- and Pe-values it is not possible to present all results of Van Leeuwen in one plot of $\langle Nu\rangle$ against Gz_L. For this reason in Fig. 7 the experimental values $\langle Nu\rangle_{exp}$, as derived from Van Leeuwen's measurements, are plotted against the theoretical values $\langle Nu\rangle_{calc}$. The theoretical values were calculated from Gz_L using equations (27). In most cases also a complete numerical calculation was carried out. As is mentioned before (Section 3.2) and as becomes clear from Figs. 4(a) and (b) the $\langle Nu\rangle$-values from both calculations are indistinguishable.

From these calculations one learns that all experimental Nusselt numbers $\langle Nu\rangle$ lie in the transition range between the two asymptotes for low and high Graetz numbers Gz_L, i.e. in the vicinity of Gz_i. Only under extreme conditions the asymptotic ranges are reached: the asymptote Nu_0 at practically stagnant flow, the asymptote $\langle Nu\rangle \propto Gz_L^{1/3}$ at high fluid velocities and extremely short probes which are almost useless for practical purposes. As a matter of fact, high Graetz numbers Gz_L are in general accompanied by

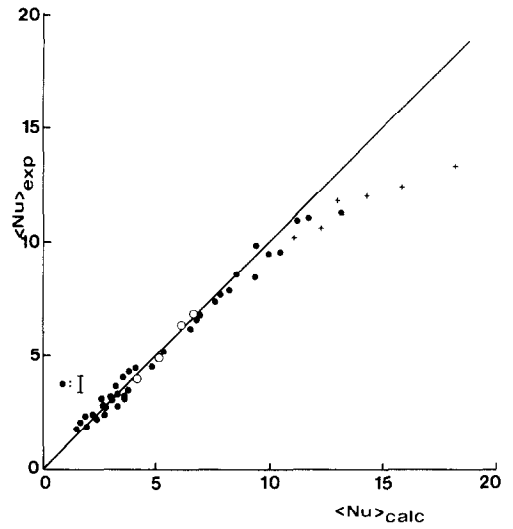

FIG. 7. Comparison of experimental and theoretical average Nusselt numbers; ●, + ... measurements by Van Leeuwen, ○ ... own measurements.

high Péclet numbers (high fluid velocities). But high Péclet numbers also cause high Nu_0-values, by which the transition range between the mentioned asymptotes is shifted to higher Gz_L-values. One can show (compare equations (23) and (26)) that one has as a first approximation $Gz_i \propto Pe^{6/5}$.

The agreement between measured and calculated values can be considered as good, if the error of the measurements is taken into account. For a number of measurements by Van Leeuwen in the range of low $\langle Nu \rangle$-values the error is known and indicated in Fig. 7. For the calculation it is assumed that the melt of the investigated polyethylene is a power-law fluid with a power-law index $n = 0.6$. With this value of the index the agreement between measured and calculated values of the average Nusselt number $\langle Nu \rangle$ is particularly good. For polyethylene $n = 0.6$ appears to be a very reasonable value (see below).

In Fig. 7 one notices six points indicated by crosses. The corresponding measurements were obtained at the highest fluid speeds available. It is not improbable that the noticed deviation of this series of points from the straight line under 45° can be ascribed to the production of additional frictional heat near the probe surface. In fact, for the highest velocity (the point most to the right in Fig. 7) a 2% decrease in Φ is sufficient to shift the $\langle Nu \rangle_{exp}$-value to the 45° line. For a temperature difference $T_2 - T_m$ of 10°C this is equivalent to a temperature increase at the tip of 0.2°C. According to the numerical calculations of Pittman and Mahmoudzadeh [4] viscous heating errors in the relevant velocity range are of the order of a few tenths of a degree centigrade.

In Fig. 7 also some points, as obtained in the laboratory of the present authors, are included. These points are indicated by open circles. These measurements were carried out with the aid of a temperature probe fitted to the tip of the torpedo of a 30 mm extruder equipped for the extrusion of pipe. This temperature probe consists of a steel tube of an external diameter of 2 mm and a wall thickness of 0.4 mm. The thermal conductivity of the steel is $k_c = 20.2\ \mathrm{J\ m^{-1}\ s^{-1}\ K^{-1}}$. The distance between the thermocouple in the tip of the probe and the downstream reference couple is 9 mm. The measurements were carried out on a low density polyethylene with a power-law index $n = 0.6$, as checked by own viscosity measurements, a thermal conductivity of $k_m = 0.23\ \mathrm{J\ m^{-1}\ s^{-1}\ K^{-1}}$, a heat capacity $c_m = 2.9 \cdot 10^3\ \mathrm{J\ kg^{-1}\ K^{-1}}$ and a density $\rho_m = 788\ \mathrm{kg\ m^{-3}}$. These data give a B-value $B = 4.45 \cdot 10^{-3}$. The measurements were carried out at relatively low fluid velocities from 0.16 to 0.72 cm s^{-1}, corresponding to Péclet numbers between 32 and 143 and Graetz numbers Gz_L between 1.8 and 8. For these measurements the agreement between experimental and theoretical $\langle Nu \rangle$-values is particularly good.

6. CONCLUSIONS AND INSTRUCTIONS

From the comparison of the measured and the calculated values of the average Nusselt number $\langle Nu \rangle$ it can be concluded that the theory developed in this paper forms a sound basis for the description of the heat transfer from a streaming polymer melt to a temperature probe consisting of a metal cylinder mounted in an upstream position.

Correct measurements of the melt temperature can only be obtained with the aid of a compensation probe [1]. Such a probe offers the possibility of determining the temperature difference $T_1 - T_2$ between the tip temperature T_1 and the adjustable reference temperature T_2 as a function of this latter temperature. For practical use, however, such a probe must be considered as rather unworkable.

Knowledge of the mechanism of heat transfer, however, opens the possibility for a calculation of the correct melt temperature from measurements with a probe containing two thermocouples, like the compensation probe, but missing the compensation facilities (for adjustment of T_2), which make the compensation probe so intricate.

The necessary calculation steps can be summarized in the following order:

(i) From κR (radius of probe cross-section), a_m and $\langle v_z \rangle$ the Péclet number Pe is calculated
(ii) With the relation $Gz_L = (\kappa R/2L)Pe$ the Graetz number Gz_L is calculated.
(iii) With the aid of the theoretical relations between $\langle Nu \rangle$ and Gz_L, which are given in graphical forms by Fig. 4, one determines the $\langle Nu \rangle$-value belonging to the Gz_L-value as calculated under (ii) and the Péclet number as calculated under (i).
(iv) With the aid of $\langle Nu \rangle$, B, Pe and Gz_L the quantity u is calculated according to $u = (BPe^2 \langle Nu \rangle)^{1/2}/Gz_L$.
(v) From Fig. 6, which gives the relation between Φ

and u, the Φ-value belonging to the calculated u-value, is derived.

(vi) The melt temperature T_m is calculated from Φ. From the definition of Φ it can easily be derived that the following equation must be used for this purpose:

$$T_m = \frac{1}{\Phi} T_1 + \left(1 - \frac{1}{\Phi}\right) T_2$$

If desired, all these steps can quickly be carried out by a suitable on-line computer.

On the basis of the theory outlined in this paper several conclusions can be drawn regarding temperature probe design and temperature errors one can expect in practice. A suitable means for the conduction error is:

$$\frac{T_1 - T_m}{T_2 - T_m} = 1 - \Phi$$

Van Leeuwen's [2] 'reduced error'.

Thus, first of all, the deviation $T_1 - T_m$ is strongly influenced by $T_2 - T_m$. For the latter temperature difference values of 10 to even 50°C are not uncommon [2, 4]. In the second place the reduced conduction error depends on $\Phi(u)$, the larger u, the larger Φ and the smaller the error. In practice u can be varied by varying the dimensions of the probe, i.e. its length L, its diameter $2\kappa R$ and its wall thickness w, and also by varying its thermal conductivity k_c. For a given probe the average melt velocity $\langle v_z \rangle$ determines u. Of the variables mentioned here, the melt velocity and the probe diameter have a modest influence: in first approximation $u \propto \langle v_z \rangle^{1/5}$ and $u \propto (\kappa R)^{-1/5}$. The influence of wall thickness and thermal conductivity is more important: $u \propto (wk_c)^{-3/5}$. Reduction of the wall thickness, although favourable from a thermal point of view, has the disadvantage of making the probe too vulnerable; $w = 0.2$ mm can be considered as a minimum value. It is also clear that it is advantageous to use a probe material of a low thermal conductivity. The greatest influence is from the length of the probe: $u \propto L$. As mentioned before, this length is limited by the restricted space available and, again, by the requirement of sufficient mechanical strengths. Lengths of 5 to 10 mm are usual.

For average melt velocities above 1 or 2 cm s^{-1} typical temperature probes produce u-values of 3 and higher (at $u = 3$, $1 - \Phi = 0.1$). This means that conduction errors at these velocities will be limited to at most a few degrees centigrade, and in most cases will be much smaller. This also follows from the finite element calculations of Pittman and Mahmoudzadeh [4] which show that at a velocity of 30 cm s^{-1}, where u is about 5 for a 5 mm probe and $1 - \Phi = 0.013$, conduction errors are negligible in comparison with viscous heating errors. At a melt velocity of 5 cm s^{-1}, using a probe of length 5 mm, radius 1 mm and wall thickness 0.2 mm, they find, after subtraction of the viscous heating contribution to the tip temperature, a reduced error of 0.01. Our theory predicts a reduced error of 0.05 in this case. The reason for this discrepancy is not yet clear.

At velocities below 1 cm s^{-1}, which are rather low but not uncommon in plastics processing, the conduction errors rapidly increase, due to the fact that below $u = 3$ the function Φ sharply decreases with u. As an example: for a probe with dimensions as mentioned before (L = 5 mm, $\kappa R = 1$ mm, $w = 0.2$ mm) the reduced error is 0.25; increasing the wall thickness to 0.4 mm leads to a reduced error of even 0.42.

As a next step in the development of the theory of the upstream temperature probe its transient behaviour must be investigated, as this behaviour is extremely important if temperature fluctuations emerge in the streaming melt or if the flow is intermittent, as is the case with injection moulding.

Also, a method should be found to include the effect of additional frictional heat, produced in the vicinity of the probe at high fluid speeds, in the present theory.

REFERENCES

1. H. Janeschitz-Kriegl, J. Schijf and J. A. M. Telgenkamp, A temperature probe for flowing polymer melts, *J. Sci. Instrum.* **40**, 415–419 (1963).
2. J. van Leeuwen, Stock temperature measurement in plastifying equipment, *Polym. Eng. Sci.* **7**, 98–109 (1967).
3. R. B. Bird, W. E. Stewart and E. N. Lightfoot, *Transport Phenomena*, 1st edn, pp. 390, 397, 325, 53. Wiley, New York (1960).
4. J. F. T. Pittman and H. Mahmoudzadeh, Performance of melt thermocouples. 2. The upstream-pointing parallel-to-flow type, *Polym. Eng. Rev.* **3**, 75–107 (1983).
5. B. Atkinson, M. P. Brocklebank, C. C. H. Card and J. M. Smith, Low Reynolds number developing flows, *AIChE J.* **15**, 548–553 (1969).
6. M. A. Lévêque, Les lois de la transmission de la chaleur par convection, *Ann. Mines* **13**, 201–299, 305–362, 381–415 (1928).
7. A. G. Fredrickson and R. B. Bird, Non-Newtonian flow in annuli, *Ind. Eng. Chem.* **50**, 347–352 (1958).
8. S. M. Richardson, Extended Lévêque solutions for flows of power law fluids in pipes and channels, *Int. J. Heat Mass Transfer* **22**, 1417–1423 (1979).
9. F. W. J. Olver, *Asymptotics and Special Functions*, 1st edn, Chapter 11. Academic Press, New York (1974).

MESURE DE TEMPERATURE ET DE TRANSFERT DE CHALEUR DANS DES POLYMERES FONDUS EN ECOULEMENT

Résumé—On donne une description théorique du transfert thermique stationnaire sur une sonde cylindrique de température plongée dans un polymère en écoulement dans une direction ascendante. Le problème est d'abord résolu numériquement pour un fluide newtonien et à loi puissance. Les nombres de Nusselt sont obtenus en fonction du nombre de Graetz locaux pour un ensemble de nombres de Péclet. A l'aide de l'expérience, des solutions analytiques approchées sont fournies pour des nombres de Graetz faibles et élevés, avec des incursions claires dans le domaine intermédiaire. Les résultats simplifiés obtenus fournissent une appréciation rapide de la validité des mesures pratiques de température. Une comparaison favorable est faite avec les résultats expérimentaux de Van Leeuven et ceux des auteurs.

TEMPERATURMESSUNG UND WÄRMEÜBERGANG IN FLIESSENDEN POLYMER-SCHMELZEN

Zusammenfassung—Es wird eine theoretische Beschreibung für die stationäre Wärmeübertragung an einer stabähnlichen Temperatur-Meßsonde wiedergegeben, die in stromaufwärtiger Richtung in eine fließende Polymer-Schmelze eingebracht wurde. Zuerst wurde das Problem numerisch für ein Newtonsches Fluid und für ein Fluid, das einem Potenzgesetz gehorcht, gelöst. Die örtliche Nusselt-Zahl wurde als eine Funktion der örtlichen Graetz-Zahl für eine Reihe von Peclet-Zahlen ermittelt. Mit Hilfe der gesammelten Erfahrung wurden analytische Näherungslösungen für niedrige und hohe Graetz-Zahlen erstellt, die im Zwischenbereicht gut übereinstimmen. Die erhaltenen vereinfachten Ergebnisse ermöglichen eine schnelle Beurteilung der Brauchbarkeit von praktischen Temperaturmessungen. Ein Vergleich mit Versuchsergebnissen von Van Leeuwen und vom Autor selbst fällt günstig aus.

ИЗМЕРЕНИЯ ТЕМПЕРАТУРЫ И ТЕПЛООБМЕНА В ДВИЖУЩИХСЯ РАСПЛАВАХ ПОЛИМЕРОВ

Аннотация—Рассмотрен стационарный теплообмен цилиндрического температурного датчика обтекаемого расплавом полимера. Первоначально задача решалась численно для ньютоновской и степенной жидкости. Для ряда чисел Пекле вычислены местные значения ччисла Нуссельта в зависимости от локальных чисел Гретца. Для малых и больших чисел Гретца получены приближенные аналитические решения, сращиваемые в промежуточном диапазоне. Они полезны для быстрых оценок в практических измерениях температуры.